JOURNAL OF Applied Polymer SCIENCE

# Preparation of polypropylene microfiltration membranes via thermally induced (solid-liquid or liquid-liquid) phase separation method

**Bo Zhou, Yuanhui Tang, Qian Li, Yakai Lin, Miao Yu, Yan Xiong, Xiaolin Wang**
Beijing Key Laboratory of Membrane Materials and Engineering, Department of Chemical Engineering, Tsinghua University, Beijing 10084, People's Republic of China
Correspondence to: X. L. Wang (E-mail: xl-wang@tsinghua.edu.cn)

**ABSTRACT:** Polypropylene (PP) hollow fiber microfiltration membranes with excellent performance were successfully prepared from the PP-binary diluent system via thermally induced liquid–liquid (L–L) phase separation method. The binary diluent consisted of myristic acid and diphenyl carbonate. The effects of the binary diluent on phase separation and membrane structure were systematically investigated. With the decrease in the weight ratio of myristic acid to diphenyl carbonate, the Flory–Huggins interaction parameter between PP and the binary diluent became more positive, and the mechanism of phase separation changed from solid–liquid (S–L) to L–L. This resulted in the membrane structure changing from spherulitic to bicontinuous. Moreover, as the weight ratio of myristic acid to diphenyl carbonate decreased from 11/9 to 2/3, the L–L phase separation region kept enlarging while the viscosity of the whole system became higher. The pore size of the cross-section increased due to the longer coarsening time while the surface pore size decreased due to the higher viscosity of the system. The bulk porosity of resultant PP membranes was mostly higher than 70% and pure water flux were generally larger than 650 L $m^{-2}$ $h^{-1}$. In addition, the PP hollow fiber microfiltration membrane possessed excellent mechanical properties (tensile strength of 3.47 MPa and elongation of 118%) and good separation performance (rejection to PEO ($M_w$ = 1000 kDa) of 94.6%) when the weight ratio of myristic acid to diphenyl carbonate was 2/3. © 2015 Wiley Periodicals, Inc. J. Appl. Polym. Sci. **2015**, *132*, 42490.

**KEYWORDS:** bicontinuous sructure; binary diluent; polypropylene; pore size; thermally induced phase separation

Received 19 March 2015; accepted 11 May 2015
**DOI: 10.1002/app.42490**

## INTRODUCTION

Polypropylene (PP) has been regarded as one of the most attractive polymers to prepare microfiltration (MF) membranes because of its excellent chemical and biological resistance, outstanding tensile strength, low cost, high temperature resistance, and easy processing.[1–3] Since PP membranes are hardly prepared via the nonsolvent-induced phase separation method due to its high stability, most industrial PP MF membranes are prepared via the dry stretch method.[4,5] The oriented elliptical pores are formed by annealing and stretching PP films, which indicates that the pore size is difficult to be controlled. Meanwhile, the porosity of obtained PP MF membranes is always <40%.[6]

Thermally induced phase separation (TIPS) method is a promising technique for preparation of the desirable PP MF membranes by controlling phase separation.[7–10] Typically, the TIPS process involves dissolving a polymer in a diluent at an elevated temperature to obtain a homogenous solution and cooling the solution for phase separation. The phase separation plays a critical role in the formation of membrane structure, which determines the separation performance and mechanical strength of the membrane.[11] Solid–liquid (S–L) phase separation usually leads to the formation of spherulitic structure while liquid–liquid (L–L) phase separation is a preferable choice to prepare membranes with bicontinuous structure which contributes to high porosity and mechanical strength.[12–14] Thus, the key point of PP membrane preparation via TIPS method involves the identification of a suitable diluent to realize L–L phase separation. However, lots of work demonstrate that PP membranes with spherulitic structure are always obtained because only S–L phase separation occurs using the majority of diluents, such as eicosane,[15] eicosanoic acid,[15] mineral oil,[16] tetradecane,[17] pentadecanoic acid,[17] dotriacontane,[17,18] soybean oil,[19–21] liquid paraffin,[22] camphene,[23,24] and chloroform.[25] Thus, it is difficult to prepare PP membranes with bicontinuous structure via TIPS method using a unary diluent. Thereby, diphenyl ether is widely used to prepare PP membranes with bicontinuous structure in spite of its unpleasant odor.[26–33]

A binary diluent composed of a primary diluent and a secondary diluent provides one more degree of freedom compared with a unary diluent. This indicates that phase separation can be manipulated by a suitable binary diluent.[34] In our preceding work, the L–L phase separation has been realized and PP membranes with bicontinuous structure have been prepared by a binary diluent.[35,36] Soybean oil which has a good compatibility with PP is used as the primary diluent while dibutyl phthalate which has a poor compatibility with PP is used as the secondary diluent. With the addition of dibutyl phthalate, the compatibility of the system becomes poor, which leads to membrane structure changing from spherulitic to bicontinuous. However, soybean oil is a mixture with five kinds of glycerol esters, which means the binary diluent actually consists of six chemicals. Thus, the interaction between PP and the binary diluent cannot be analyzed without difficulty, and the L–L phase separation region of the system can hardly be controlled. Moreover, only irregular pore size can be obtained due to the complicated binary diluent.

This study aims to investigate the effect of the binary diluent on phase separation and membrane structure systematically and to prepare PP MF membranes with excellent performance by the binary diluent. Myristic acid and diphenyl carbonate are used as the primary diluent and secondary diluent, respectively. First, the effect of the weight ratio of myristic acid to diphenyl carbonate on phase separation is investigated. The Flory–Huggins interaction parameter between PP and the binary diluent is calculated to reflect the interaction between PP and the binary diluent as well as to predict the mechanism of phase separation. The thermodynamic phase diagrams of PP-binary diluent systems are plotted to analyze the phase separation of different systems. Then PP hollow fiber MF membranes with bicontinuous structure are prepared via TIPS (L–L) method using the binary diluent. Effects of the L–L phase separation region and the viscosity of the system on membrane structure and performance are investigated in detail.

## EXPERIMENTAL

### Materials

Polypropylene (PP, MI = 1.4 g/10 min) was provided by Samsung Total. Myristic acid ($M_w$ = 228.37 Da), diphenyl carbonate ($M_w$ = 214.22 Da), and polyethylene oxide (PEO, $M_w$ = 1000 kDa) were purchased from Sinopharm Chemical Reagent Co., Ltd.

### Determination of Phase Diagram

The cloud point temperature of the PP-binary diluent system was defined as the temperature below which the solution became turbid. It was obtained by an optical microscopy (Olympus BX51). The blend sample of PP and binary diluent was prepared via previously described method.[37,38] Then the sample was sandwiched between a pair of glass microscope coverslips, which were sealed with silicone rubber to prevent evaporation of the diluent. Finally, the sample was placed on a hot stage (Linkam THMS 600) at 180°C for 5 min and cooled to 50°C at the rate of 10°C/min.

The crystallization temperature was determined by differential scanning calorimetry (DSC, TA Q200). The blend sample of the PP-binary diluent system was melted at 180°C for 5 min, and then cooled to 50°C at the rate of 10°C/min. The peak of the DSC curve was regarded as the crystallization temperature.

**Table I.** Preparation Conditions of PP Membranes

| Sample ID | PP concentration (wt %) | Weight ratio of myristic acid to diphenyl carbonate |
|---|---|---|
| S1 | 20 | 1/0 |
| S2 | 20 | 4/1 |
| S3 | 20 | 7/3 |
| S4 | 20 | 3/2 |
| S5 | 20 | 11/9 |
| S6 | 20 | 1/1 |
| S7 | 20 | 9/11 |
| S8 | 20 | 2/3 |

### Preparation of PP Membranes

The PP hollow fiber membranes were prepared from PP-binary diluent systems via TIPS method. The binary diluent consisted of myristic acid and diphenyl carbonate. PP, myristic acid, and diphenyl carbonate powder with certain concentrations were melt-blended in a twin-screw extruder at an elevated temperature (150–190°C) to obtain a homogenous dope solution. The temperature of the spinneret at the end of extruder was 150°C. The dope solution was extruded from the spinneret and then immersed into a water bath at 50°C to induce phase separation. The dope flow rate was 16.7 g/min. The air gap between the spinneret and the water bath was 2 mm. After that, the solidified hollow fiber membrane was wound on a take-up roller. The take-up speed was 48 m/min. Glycerol was employed as bore liquid at 180°C and the bore flow rate was 9 g/min. The diluent in the membrane was extracted by ethanol and the PP hollow fiber membrane was obtained after the volatilization of ethanol. The preparation conditions of hollow fiber membranes were listed in Table I.

### Characterization of PP Membranes

**Morphologies.** The morphologies of PP hollow fiber membranes were examined using a scanning electron microscope (SEM, JEOL JSM7401). PP hollow fiber membranes were fractured in liquid nitrogen and coated with platinum. The SEM with the accelerating voltage of 3.0 kV was used to examine cross-section and surface morphologies of membranes.

**Mechanical Properties.** The mechanical strength of the hollow fiber membrane was measured via a universal testing machine (Shimadzu AGS-100A) equipped with a 5 kg load cell. Each sample was stretched at a constant rate of 25 mm/min. The initial distance between the clamps was of 50 mm. To eliminate the randomness, 5 specimens were tested for each sample.

**Crystallinity.** The melting curve was carried out on a TA Instruments Q-200 DSC in a dry nitrogen atmosphere. PP membranes were sealed in an aluminum pan, which was heated to 200°C at a rate of 10°C/min. The crystallinity ($X_c$) of PP membrane was calculated by the following equation:

**Table II.** Properties of PP and Diluents

| Materials | $V^a$ ($cm^3$/mol) | $\delta_d$ ($MPa^{1/2}$) | $\delta_p$ ($MPa^{1/2}$) | $\delta_h$ ($MPa^{1/2}$) | $\delta$ ($MPa^{1/2}$) | $\chi^d$ |
|---|---|---|---|---|---|---|
| PP | - | 18.00[b] | 0[b] | 1.00[b] | 18.03 | - |
| Myristic acid | 254.2 | 16.48[c] | 1.65[c] | 6.27[c] | 17.71 | 0.35 |
| Diphenyl carbonate | 178.9 | 18.73[c] | 3.64[c] | 7.48[c] | 20.49 | 0.77 |

$V$, molar volume; $\delta$, solubility parameter at 25°C; $\chi$, Flory–Huggins interaction parameter between PP and the diluent at 25°C.
[a] $V$ calculated using Advanced Chemistry Development (ACD/Labs) Software V11.02 (© 1994–2014 ACD/Labs).
[b] Data from Ref. 58.
[c] Data estimated by group contribution methods.[59]
[d] $\chi$ can be related to $\delta$: $\chi = 0.34 + V_1(\delta_1 - \delta_2)^2/RT$, where 1 and 2, respectively, denote diluent and polymer.[59]

$$X_c = \Delta H_f / \Delta H_{f,0} \times 100\%$$

Where $\Delta H_f$ is the fusion enthalpy of the precursor and $\Delta H_{f,0}$ is 209 J/g,[39] the fusion enthalpy of 100% crystalline PP.

**Average Pore Size and Pore Size Distribution.** The pore size and pore size distribution were determined by analyzing SEM images using the software Image-Pro Plus 6.0 as reported in Ref. 40.

**Bulk Porosity and Surface Porosity.** The bulk porosity of the PP hollow fiber membrane $\varepsilon_{bulk}$ was measured through the determination of the amount of isobutanol absorbed by the membranes using the following equation:[12]

$$\varepsilon_{bulk} = (m_1 - m_2)/\rho_i / ((m_1 - m_2)/\rho_i + m_2/\rho_p)$$

where $m_1$ is the weight of the wet membrane (g); $m_2$ is the weight of the dry membrane (g); $\rho_i$ is the isobutanol density (0.806 g·$cm^{-3}$), and $\rho_p$ is the polymer density (0.891 g·$cm^{-3}$).

The surface porosity $\varepsilon_{surface}$ was determined by analyzing SEM images using the software Image-Pro Plus 6.0. In this case, the porosity was determined directly by comparing the area of dark regions (the pores) and light regions (the polymer) as reported in Ref. 41.

**Filtration Performance.** The pure water flux and rejection of the hollow fiber membrane were determined using a self-made dead-end filtration under the pressure of 0.1 MPa. The flux ($J_v$) was calculated according to the following equation:[42]

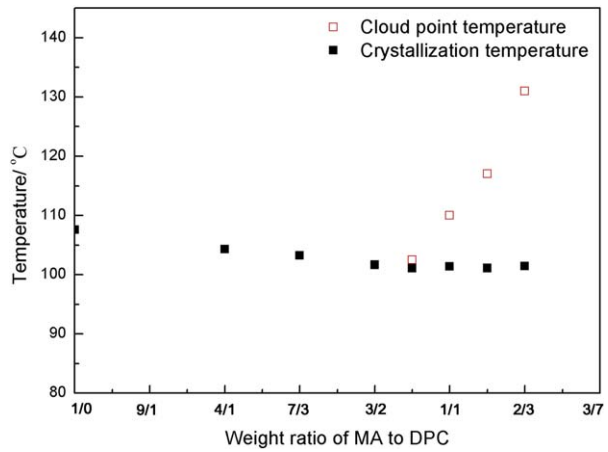


**Figure 1.** Phase diagram for the PP-binary diluent systems with various weight ratios of myristic acid to diphenyl carbonate at the PP concentration of 20 wt %. [Color figure can be viewed in the online issue, which is available at wileyonlinelibrary.com.]

$$J_v = m/(\rho \cdot A \cdot \Delta t)$$

Where $m$, $\rho$, $A$, and $\Delta t$ are the permeation mass (g), water density (g/L), outside surface area of the membrane ($m^2$), and permeation time (h), respectively.

The same setup was used for rejection experiments with PEO ($M_w$ = 1000 kD) at the concentration of 2 g/L. The concentrations of PEO in the feed and permeation solutions were analyzed via total organic carbon. The rejection ($R$) was calculated by the following equation:

$$R = (1 - C_P/C_F)$$

Where $C_P$ and $C_F$ are the protein concentrations in the permeation and feed solutions after the cyclic filtration, respectively.

## RESULTS AND DISCUSSION

### Phase Diagram

The L–L phase separation can be directly realized if a suitable binary diluent is used.[43–46] Generally, the primary diluent is the one that has good compatibility with the polymer.[35,36,47] In this work, myristic acid is selected as the primary diluent because of

**Table III.** Flory–Huggins Interaction Parameters Between PP and Binary Diluents

| Weight ratio of myristic acid to diphenyl carbonate | $V_B$[a] ($cm^3$/mol) | $\delta_B$[b] ($MPa^{1/2}$) | $X$ |
|---|---|---|---|
| 1/0 | 254.2 | 17.71 | 0.35 |
| 4/1 | 242.3 | 18.15 | 0.34 |
| 7/3 | 235.9 | 18.39 | 0.35 |
| 3/2 | 229.1 | 18.64 | 0.37 |
| 11/9 | 225.6 | 18.77 | 0.39 |
| 1/1 | 221.9 | 18.90 | 0.41 |
| 9/11 | 218.2 | 19.04 | 0.43 |
| 2/3 | 214.3 | 19.18 | 0.45 |
| 7/13 | 210.4 | 19.33 | 0.48 |

$V_B$, molar volume of binary diluent; $\delta_B$, solubility parameter of binary diluent at 25°C.
[a] $V_B = \varphi_i V_i + \varphi_j V_j$, where $\varphi_i$ and $\varphi_j$, respectively, are the volume fraction of myristic acid and diphenyl carbonate; $i$ and $j$, respectively, denote the myristic acid and diphenyl carbonate.
[b] $\delta_B = \varphi_i \delta_i + \varphi_j \delta_j$, where $\varphi_i$ and $\varphi_j$, respectively, are the volume fraction of myristic acid and diphenyl carbonate; $i$ and $j$, respectively, denote the myristic acid and diphenyl carbonate.

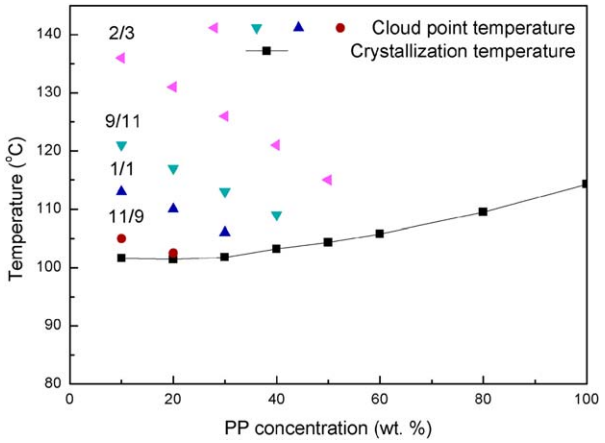


**Figure 2.** Phase diagram for the PP-binary diluent systems with various weight ratios of myristic acid to diphenyl carbonate. [Color figure can be viewed in the online issue, which is available at wileyonlinelibrary.com.]

its low Flory–Huggins interaction parameter ($\chi$) with PP (seen in Table II). In order to obtain L–L phase separation, diphenyl carbonate that has poor compatibility with PP is added into the PP–myristic acid system to alter the interaction of the system.

Phase diagram for PP-binary diluent systems with various weight ratios of myristic acid to diphenyl carbonate at the PP concentration of 20 wt % is shown in Figure 1. When the weight ratio of myristic acid to diphenyl carbonate is more than 3/2, only S–L phase separation is observed and the crystallization temperature slightly decreases. As the weight ratio decreases to 11/9, the mechanism of the phase separation changes from S–L phase separation to L–L phase separation with the subsequent polymer crystallization. With the continuous decrease of the weight ratio, the gap between the cloud point temperature and the crystallization temperature becomes larger while the crystallization temperature remains unchanged.

The overall feature in Figure 1 can be analyzed in terms of the interaction between PP and the binary diluent. The Flory–Huggins interaction parameter ($\chi$), typically used to interpret the interaction between the polymer and the diluent, is calculated from the differences of the solubility parameters between PP and the binary diluent as listed in Table III. The solubility parameter ($\delta$) of the binary diluent increases as the weight ratio of myristic acid to diphenyl carbonate decreases, which results in a more positive $\chi$. When the weight ratio of myristic acid to diphenyl carbonate is more than 3/2, the Flory–Huggins interaction parameter value is relatively small (lower than 0.37), which indicates good compatibility of the system. Thus only S–L phase separation occurs. Meanwhile, it has been reported that the addition of "poor" solvents increases the viscosity, since polymer chains form a network, which prevents the polymer chains from flowing.[48,49] Thus, the mobility of PP segments decreases with the addition of diphenyl carbonate, preventing crystal nucleation and growth of PP.[50–52] Therefore, the system needs deeper degree of super cooling to form crystal nuclei of PP and the crystallization temperature decreases as the weight ratio of myristic acid to diphenyl carbonate decreases. Furthermore, the Flory–Huggins interaction parameter value continually increases as the weight ratio of myristic acid to diphenyl carbonate changes from 11/9 to 2/3. This means that the Gibbs free energy of mixing $\triangle G_{mix}$ becomes positive and demixing would occur.[53] Thus, the L–L phase separation region is enlarged. Finally, the homogenous solution cannot be obtained at an elevated temperature as the weight ratio of myristic acid to diphenyl carbonate is 7/13 due to the much poorer compatibility of the PP-binary diluent system.

The phase diagram for the PP-binary diluent systems with the weight ratios of myristic acid to diphenyl carbonate from 11/9 to 2/3 is shown in Figure 2. A typical upper critical solution temperature type phase behavior is shown. As reported, the monotectic point $\varphi_m$ increases as $\chi$ increases.[53] As the weight ratio of myristic acid to diphenyl carbonate ranges from 11/9 to 2/3, the monotectic point $\varphi_m$ increases from 20 to 60%, indicating a fast extend of the L–L phase separation region. On the other hand, the crystallization temperature is barely influenced by varying the weight ratio of myristic acid to diphenyl carbonate as shown in Figure 1. The fluctuation of the crystallization

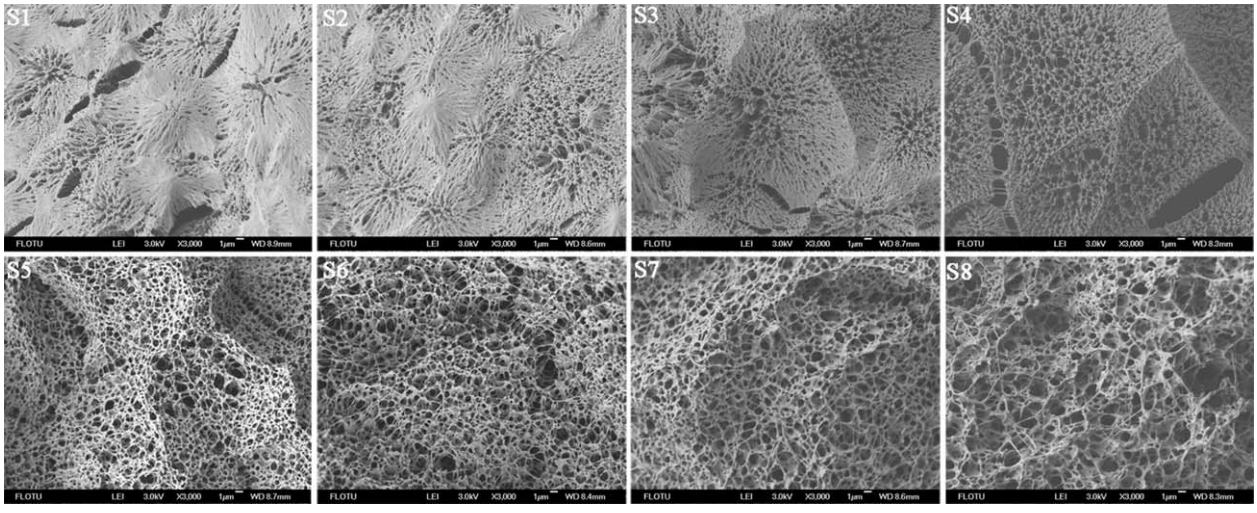


**Figure 3.** Cross-section morphologies of PP membranes (magnification: 3000×).

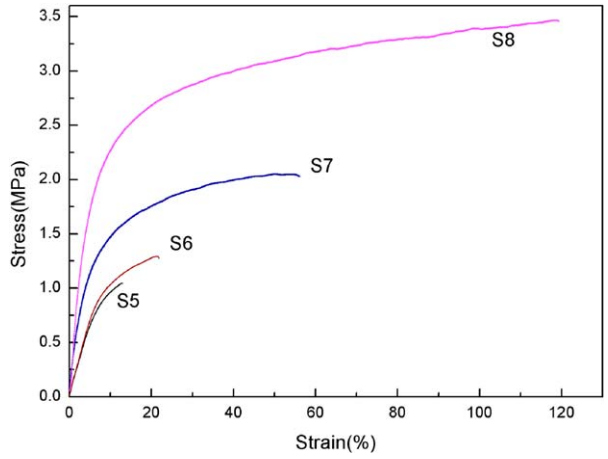


**Figure 4.** Stress–strain curves of PP membranes. [Color figure can be viewed in the online issue, which is available at wileyonlinelibrary.com.]

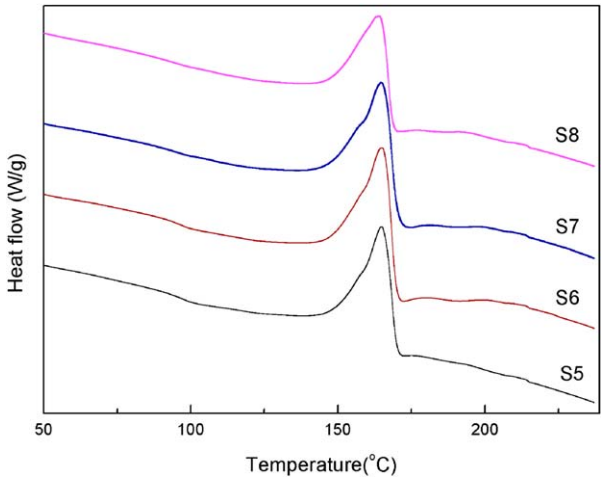


**Figure 5.** DSC melting curves of PP membranes. [Color figure can be viewed in the online issue, which is available at wileyonlinelibrary.com.]

temperature at a fixed PP concentration is <1%. Therefore, the crystallization temperatures in Figure 2 are obtained by averaging the several crystallization temperatures of various weight ratios of myristic acid to diphenyl carbonate. Nevertheless, the crystallization temperature slightly increases by increasing the PP concentration. As reported, the addition of diluent lowers the chemical potential of the polymer in the solution.[54,55] So addition of the binary diluent here also lowers the chemical potential, leading to the depression of the crystallization temperature of PP. Meanwhile, the lower crystallization temperature of the system indicates a higher degree of supercooling or a larger driving force needed for polymer crystallization.[56] This suggests that larger driving force is needed for PP crystallization with the increase in the weight ratio of myristic acid to diphenyl carbonate.

The result of the phase diagram demonstrates that the mechanism of phase separation has been altered by changing the composition of the binary diluent and the L–L phase separation region can be continuously manipulated. Additionally, myristic acid to diphenyl carbonate can be conveniently recycled by recrystallization with low energy consumption since it is solid around room temperature,[57] which indicates a more environmental and cost-effective membrane preparation process.

### Cross-Section Morphologies

The evolution in the structure of membrane preparation via TIPS method is closely related to the thermodynamics of the phase separation process.[60] As shown in Figure 2, with the decrease of the polymer concentration, the gap between the cloud temperature and the crystallization temperature is larger, which suggests that the enhanced effect of the L–L phase separation on membrane structure can be easily analyzed. Nevertheless, it is difficult to prepare membranes with the much lower polymer concentration due to lower viscosity of polymer solution. Thus, the effect of thermodynamics of the phase separation process on membrane structure is investigated at the polymer concentration of 20 wt % in the following section.

Cross-section morphologies of PP hollow fiber membranes prepared by various weight ratios of myristic acid to diphenyl carbonate are shown in Figure 3. When the weight ratio of myristic acid to diphenyl carbonate is more than 3/2, the PP-binary diluent system undergoes the S–L phase separation, which has been illustrated in Figure 1. Thus, the cross-section structure of resultant membranes is mainly spherulitic as shown in Figure 3. With the decrease in the weight ratio of myristic acid to diphenyl carbonate, the spherulites become bigger. This is attributed to the weaker interaction between PP and the binary diluent which prevents the nucleation activity of PP and leads to the formation of fewer primary nuclei at the beginning of crystallization as well as the lower crystallization temperature (Figure 1).

When the weight ratio of myristic acid to diphenyl carbonate ranges from 11/9 to 2/3, the interaction between PP and binary diluent becomes weaker and the L–L phase separation occurs. The system enters an unstable or a metastable region. The phase

**Table IV.** Mechanical Properties of PP Membranes

| Sample ID | Modulus (MPa) | Tensile strength (MPa) | Elongation at break (%) |
|---|---|---|---|
| S1–S4 | – | – | Almost no elongation |
| S5 | 12.9 | 1.05 | 12.9 |
| S6 | 13.5 | 1.29 | 21.5 |
| S7 | 25.3 | 2.05 | 50.2 |
| S8 | 49.7 | 3.47 | 118 |

**Table V.** The Fusion Enthalpy and Crystallinity of PP Membranes

| Sample ID | $\Delta H_f$ (J/g) | $X_c$ (%) |
|---|---|---|
| S5 | 104.1 | 49.8 |
| S6 | 93.94 | 44.9 |
| S7 | 85.24 | 40.8 |
| S8 | 75.01 | 35.9 |

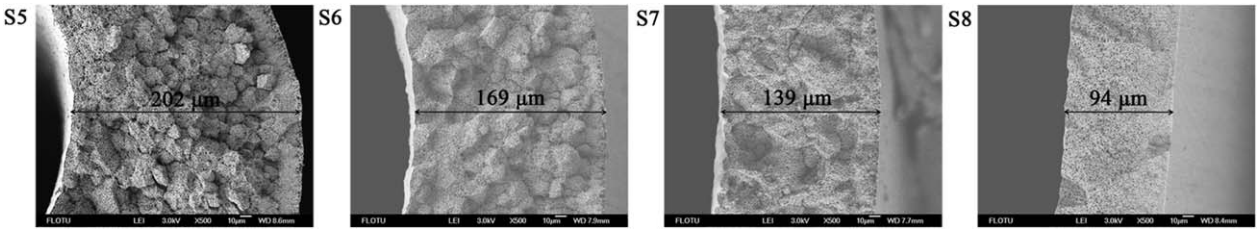


**Figure 6.** Thicknesses of PP membranes (magnification: 500×).

separation proceeds through nucleation and growth in the metastable region, whereas it occurs through spinodal decomposition in the unstable region. The system is divided to two phases, namely, rich-polymer phase and lean-polymer phase. Then the rich-polymer phase solidifies and the structure is formed when the temperature of the system is below the crystallization temperature. In this case, the resulting phase separation process is determined by spinodal decomposition. Phase separation proceeds instantaneously and results initially in a regular, highly interconnected structure. When the weight ratio of myristic acid to diphenyl carbonate is 11/9, the cloud point temperature of the system is close to the crystallization temperature. In the cooling process, since the L–L phase separation occurs almost simultaneously with polymer crystallization, the resultant membrane exhibits the structure mixed of spherulitic and bicontinuous structure. With the decrease in the weight ratio of myristic acid to diphenyl carbonate, the region between the cloud point curve and crystallization curve becomes larger. As a consequence, the phase separation of spinodal decomposition occurs far before polymer crystallization. Therefore, the spherulitic structure disappears gradually and is replaced by the uniform bicontinuous structure. In short, the cross-section morphologies of the PP membranes can be significantly altered by the mechanism of phase separation and the L–L phase separation region.

### Mechanical Properties

It is well known that the cross-section morphologies play an important role on the mechanical properties of the membranes.[61,62] Figure 4 describes the stress–strain curves of PP hollow fiber membranes prepared at the PP concentration of 20 wt % by various weight ratios of myristic acid to diphenyl carbonate. Specific values of the mechanical properties of membranes are summarized in Table IV. It should be noted that when the weight ratio of myristic acid to diphenyl carbonate decreases from 1/0 to 3/2, the resultant membranes (S1–S4) are brittle and have little elongation due to the spherulitic structure, which demonstrates that the membranes (S1–S4) are difficult to characterize. With the continuous decrease in the weight ratio, the structure of the resultant membranes changes from spherulitic to bicontinuous. The tensile strength and elongation of the resultant membranes (S5–S8) with bicontinuous structure are above 1 MPa and 10%, respectively, due to the better connectivity. The membrane S8 prepared with 2/3 weight ratio of myristic acid to diphenyl carbonate has the highest tensile strength (3.47 MPa) and elongation (118%). It is attributed to the uniform bicontinuous structure. This interconnected structure leads to the much more conductive plastic flow under applied stress, thereby delaying crack formation.

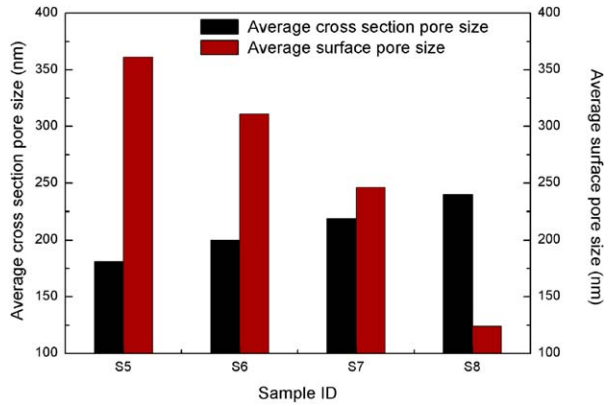


**Figure 7.** Average pore sizes of PP membranes. [Color figure can be viewed in the online issue, which is available at wileyonlinelibrary.com.]

Bicontinuous structure contributes to high tensile strength which is needed for characterization of PP membranes. Thus, only the membranes (S5–S8) with bicontinuous structure are analyzed systematically to investigate the phase separation on the PP membrane performance in the following section.

### Thermal and Crystalline Properties

As mentioned above, when the weight ratio of myristic acid to diphenyl carbonate ranges from 11/9 to 2/3, the L–L phase separation occurs, followed closely by polymer crystallization. The crystallization of the PP membrane is investigated by DSC. DSC melting curves of the PP hollow fiber membranes prepared at the PP concentration of 20 wt % by various weight ratios of myristic acid to diphenyl carbonate are shown in Figure 5. As the weight ratio of myristic acid to diphenyl carbonate decreases, the melting curve shows only one wide temperature peak at about 165°C. There is no obvious change in peak temperature and the shape of the melting curve, indicating the addition of diphenyl carbonate does not induce the formation of a new crystal phase. Meanwhile, the fusion enthalpy and crystallinity of PP membranes prepared by varying the weight ratio of myristic acid to diphenyl carbonate are summarized in Table V. PP membranes with spherulitic structure have higher fusion enthalpy and crystallinity.

The overall feature of the membrane crystallization can be analyzed by the change of viscosity of the PP-binary diluent system, which strongly affects regular folding of polymer molecules in the crystallization process.[52] As reported, the addition of "poor" solvents increases the viscosity, since polymer chains form a network, which prevents the polymer chains from flowing.[48,49] The

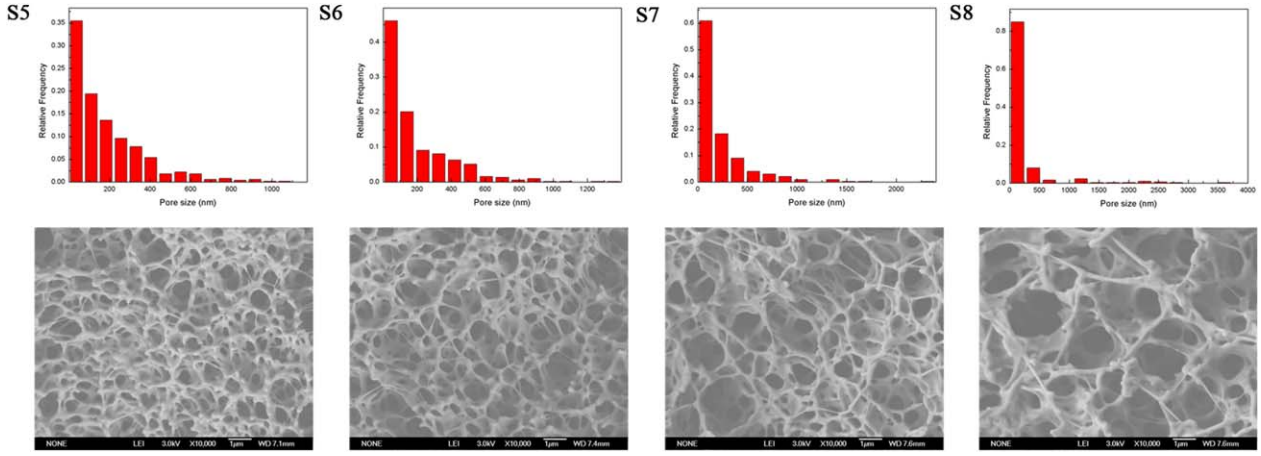


**Figure 8.** Cross-section morphologies and pore size distributions of PP membranes (magnification: 10,000×). [Color figure can be viewed in the online issue, which is available at wileyonlinelibrary.com.]

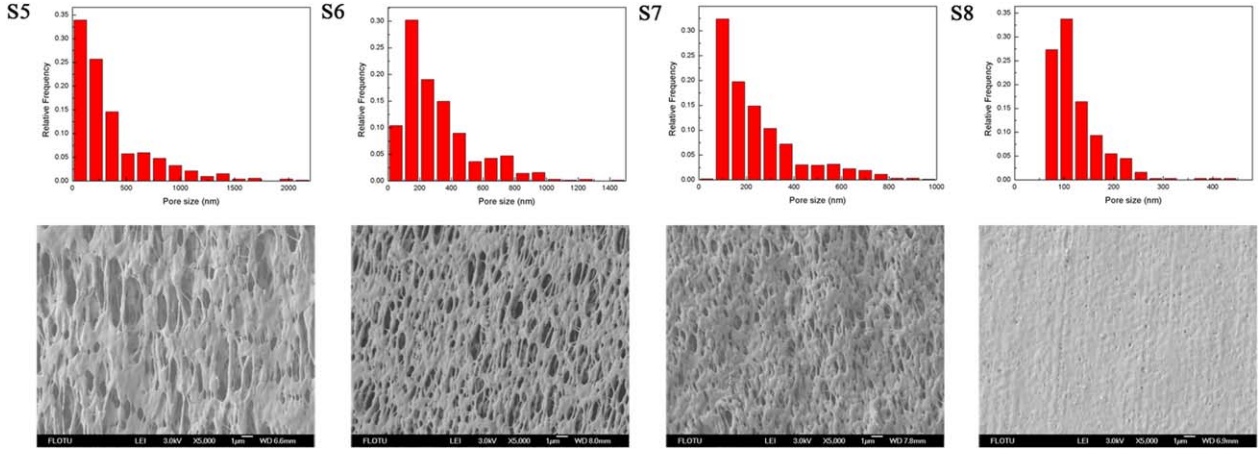


**Figure 9.** Surface morphologies and pore size distributions of PP membranes (magnification: 10,000×). [Color figure can be viewed in the online issue, which is available at wileyonlinelibrary.com.]

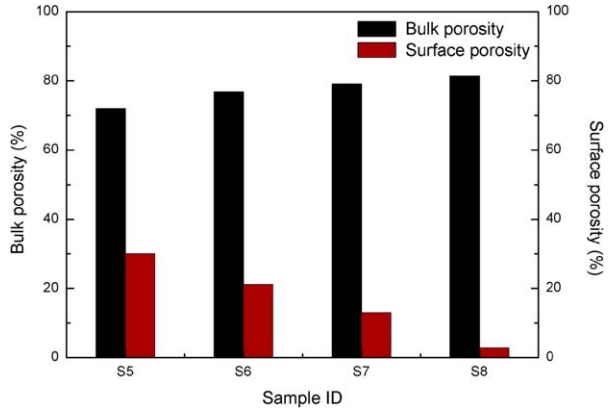


**Figure 10.** Porosities of PP membranes. [Color figure can be viewed in the online issue, which is available at wileyonlinelibrary.com.]

change of the viscosity of the PP-binary diluent system can also be verified by the variation of the membrane thickness. As shown in Figure 6, the membrane thickness decreases with the addition of the "poor" diluent (diphenyl carbonate). This means the extrusion of the PP-binary diluent system becomes more difficult, which implies the higher viscosity of the PP-binary diluent system. Meanwhile, it has been reported that higher viscosity prevents the regular folding of polymer molecules in the crystallization process, which results in the decrease in the crystallinity.[50,52] Thus, with the decrease in the weight ratio of myristic acid to diphenyl carbonate, mobility of PP segments decreases, preventing crystal nucleation and growth of PP.

### Average Pore Size, Pore Size Distribution, and Porosity

The filtration performance of the PP membrane is determined by the average pore size, pore size distribution, and porosity. The average pore size of PP membranes prepared at the PP concentration of 20 wt % by various weight ratios of myristic acid to diphenyl carbonate are shown in Figure 7. The pore size distributions of the PP membranes prepared at the PP concentration of 20 wt % by various weight ratios of myristic acid to diphenyl carbonate are shown in Figures 8 and 9. With the

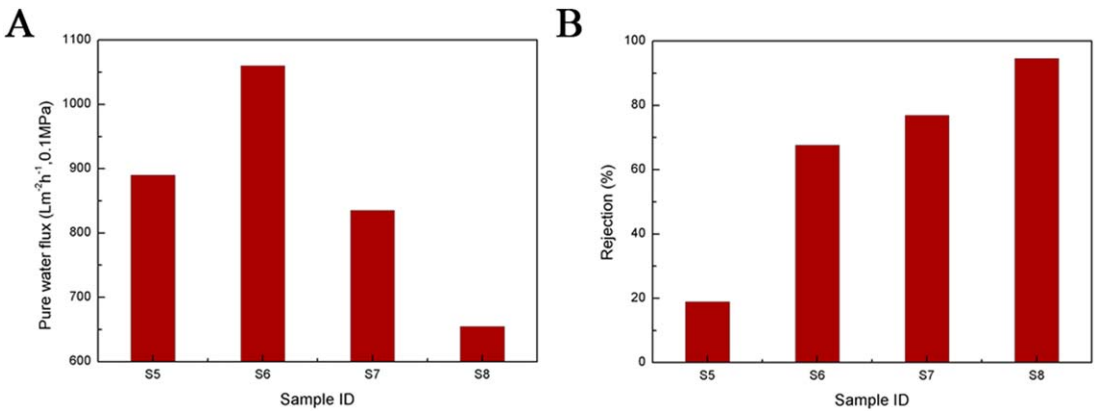


**Figure 11.** Pure water flux and rejection of PP membranes. [Color figure can be viewed in the online issue, which is available at wileyonlinelibrary.com.]

decrease in the weight ratio of myristic acid to diphenyl carbonate, the cross-section pore size increases from 181 to 240 nm while surface pore size decreases from 361 to 124 nm.

The pore size mainly depends on the droplet growth. When the weight ratio of myristic acid to diphenyl carbonate ranges from 11/9 to 2/3, the resulting phase separation is determined by spinodal decomposition. Then the two-phase system will continue to evolve in response to its tendency to reduce the surface energy associated with interfacial area. The coarsening process has been interpreted by three different mechanisms: ostwald ripening, coalescence, and the hydrodynamic flow mechanism. All the mechanisms present that droplet growth is closely related to the coarsening time and viscosity.[60,63] With the decrease in the weight ratio of myristic acid to diphenyl carbonate, the L–L phase separation region gets wider. As a result, the L–L phase separation occurs at the higher temperature while the system solidifies around the similar temperature, which leads to the longer coarsening time for droplet growth under identical cooling process. Thus, the pore size of the membrane cross-section increases. Nevertheless, polymer solution near the surface rapidly solidifies at the moment entering to the water bath. Thus the coarsening time is similar although the weight ratio of myristic acid to diphenyl carbonate is changed. In this case, the viscosity plays a more critical role in droplet growth.[45,46] The viscosity of the system increases with the decrease in the weight ratio of myristic acid to diphenyl carbonate, resulting in the decrease in the diffusivity of the diluent. This hinders the rapid growth of the droplet. Thus the surface pore size decreases with the decrease in the weight ratio of myristic acid to diphenyl carbonate.

The bulk and surface porosities of PP membranes prepared at the PP concentration of 20 wt % by various weight ratios of myristic acid to diphenyl carbonate are shown in Figure 10. The bulk porosities of all four PP membranes are higher than 70%, indicating good permeability. With the decrease of the weight ratio of myristic acid to diphenyl carbonate, the bulk porosity increases gradually. As reported, more crystallites would push more diluent outside of membrane, thus decreasing the porosity of the membrane.[64] As a result, the membrane with bicontinuous structure and lower crystallinity has the higher bulk porosity. On the contrary, with the decrease of the weight ratio of myristic acid to diphenyl carbonate, the surface porosity reduces greatly from 30 to 2.8%, which results from the simultaneous decrease of the pore number and the pore size.

### Filtration Performance

Pure water flux and rejection to PEO ($M_w = 1000$ kDa) of PP hollow fiber membranes prepared at the PP concentration of 20 wt % by various weight ratios of myristic acid to diphenyl carbonate are shown in Figure 11. The pure water flux is both influenced by bulk porosity and surface porosity. Four PP hollow fiber membranes have large pure water flux above 650 L $m^{-2}$ $h^{-1}$, which is much higher than that of the relative reference.[43] The pure water flux increases firstly with the decrease in the weight ratio of myristic acid to diphenyl carbonate due to the higher bulk porosity. Then the pure water flux decreases due to the reduction in surface porosity. The membrane S6 has the considerable pure water flux of 1060 L $m^{-2}$ $h^{-1}$.

Rejection is mainly influenced by surface pore size.[65] The membrane S5 has many big pores on its surface, which is much larger than diameter of PEO ($M_w = 1000$ kDa). Thereby, the rejection is as low as 18.9%. With the decrease in the weight ratio of myristic acid to diphenyl carbonate, the surface pore size decrease and big pores disappear, which indicates a fast increase of the rejection. When the weight ratio of myristic acid to diphenyl carbonate is 2/3, the rejection of the resultant membrane is as high as 94.6%.

In short, the reduction of the weight ratio of myristic acid to diphenyl carbonate increases the bulk porosity and decreases the surface porosity and pore size. As the weight ratio of myristic acid to diphenyl carbonate is 2/3, the pure water flux and rejection to ($M_w = 1000$ kDa) are 655 L $m^{-2}$ $h^{-1}$ and 94.6%, indicating an excellent MF performance.

## CONCLUSIONS

PP MF membranes are prepared from the PP-binary diluent system via TIPS method using the binary diluent of myristic acid to diphenyl carbonate. As the weight ratio of myristic acid to diphenyl carbonate decreases, the mechanism of phase separation changes from S–L to L–L. The PP membranes with

bicontinuous structure are successfully prepared. Meanwhile, the membrane porosity and pore size can be continuously manipulated by varying the weight ratio of myristic acid to diphenyl carbonate due to the change of L–L phase separation region and viscosity of the system. As the weight ratio of myristic acid to diphenyl carbonate is 2/3, the PP hollow fiber MF membrane with excellent mechanical properties (tensile strength of 3.47 MPa and elongation of 118%) and filtration performance (pure water flux of 655 L $m^{-2}$ $h^{-1}$ and rejection to PEO ($M_w = 1000$ kDa) of 94.6%) is prepared. The conclusions are also beneficial to the preparation of other polymer membranes with excellent performance. Nevertheless, the final membrane structure also depends on the kinetics of the phase separation process. In the future work, the kinetics of the L–L phase separation and the subsequent polymer crystallization as well as its effect on membrane formation will be investigated to further improve the performance of PP MF membranes.

## ACKNOWLEDGMENTS

The authors would like to thank National Key Technologies R&D Program of China (No. 2015BAE06B00) and Tsinghua University Initiative Scientific Research Program (20121088039).

## REFERENCES

1. Chen, L.; Ma, C. G.; Wang, H. Y.; Zhang, J. X.; Xiong, X. M. *J. Appl. Polym. Sci.* **2015**, *132*, 41685.
2. Ding, Z.; Bao, R.; Zhao, B.; Yan, J.; Liu, Z.; Yang, M. *J. Appl. Polym. Sci.* **2013**, *130*, 1659.
3. Gorouhi, E.; Sadrzadeh, M.; Mohammadi, T. *Desalination* **2006**, *200*, 319.
4. Yan, S.; Xiao, X.; Huang, X.; Li, X.; Qi, Y. *Polymer* **2014**, *55*, 6282.
5. Saffar, A.; Carreau, P. J.; Ajji, A.; Kamal, M. R. *Ind. Eng. Chem. Res.* **2014**, *53*, 14014.
6. Offord, G. T.; Armstrong, S. R.; Freeman, B. D.; Baer, E.; Hiltner, A.; Swinnea, J. S.; Paul, D. R. *Polymer* **2013**, *54*, 2577.
7. Castro, A. J. U.S. Patent 4,247,498, **1981**.
8. Matsuyama, H.; Berghmans, S.; Lloyd, D. R. *Polymer* **1999**, *40*, 2289.
9. Matsuyama, H.; Kim, M.-m.; Lloyd, D. R. *J. Membr. Sci.* **2002**, *204*, 413.
10. Ding, H. Y.; Zeng, Y. M.; Meng, X. F.; Tian, Y.; Shi, Y. Q.; Jiao, Q. Z.; Zhang, S. M. *J. Appl. Polym. Sci.* **2006**, *102*, 2959.
11. Liu, M.; Chen, D. G.; Xu, Z. L.; Wei, Y. M.; Tong, M. *J. Appl. Polym. Sci.* **2013**, *128*, 836.
12. Lin, Y. K.; Tang, Y. H.; Ma, H. Y.; Yang, J.; Tian, Y.; Ma, W. Z.; Wang, X. L. *J. Appl. Polym. Sci.* **2009**, *114*, 1523.
13. Shan, M. X.; Matsuyama, H.; Teramoto, M.; Okuno, J.; Lloyd, D. R.; Kubota, N. *J. Appl. Polym. Sci.* **2005**, *95*, 219.
14. Ji, G. L.; Zhu, L. P.; Zhu, B. K.; Zhang, C. F.; Xu, Y. Y. *J. Membr. Sci.* **2008**, *319*, 264.
15. Kim, S. S.; Lloyd, D. R. *J. Membr. Sci.* **1991**, *64*, 13.
16. Lim, G. B. A.; Kim, S. S.; Ye, Q. H.; Wang, Y. F.; Lloyd, D. R. *J. Membr. Sci.* **1991**, *64*, 31.
17. Kim, S. S.; Lim, G. B. A.; Alwattari, A. A.; Wang, Y. F.; Lloyd, D. R. *J. Membr. Sci.* **1991**, *64*, 41.
18. McGuire, K. S.; Lloyd, D. R.; Lim, G. B. A. *J. Membr. Sci.* **1993**, *79*, 27.
19. Kim, J. J.; Hwang, J. R.; Kim, U. Y.; Kim, S. S. *J. Membr. Sci.* **1995**, *108*, 25.
20. Iqbal, N.; Ahmad, N. M.; Sagar, S.; Iqbal, F.; Tareen, M. H. K.; Khan, T. A.; Mehfooz, S.; Khan, M. B.; Jameel, T. *J. Appl. Polym. Sci.* **2013**, *130*, 2821.
21. Tang, N.; Jia, Q.; Zhang, H.; Li, J.; Cao, S. *Desalination* **2010**, *256*, 27.
22. Gu, B.; Cao, Y.; Du, Q. G.; Yang, Y. L. *Polym. Bull.* **1999**, *43*, 291.
23. Yang, M. C.; Perng, J. S. *J. Polym. Res.-Taiwan* **1999**, *6*, 251.
24. Yang, M. C.; Perng, J. S. *J. Membr. Sci.* **2001**, *187*, 13.
25. Lu, Y.; Tan, K.; Sun, A.; Li, C.; Wang, Z. *J. Appl. Polym. Sci.* **2009**, *111*, 3050.
26. Matsuyama, H.; Okafuji, H.; Maki, T.; Teramoto, M.; Tsujioka, N. *J. Appl. Polym. Sci.* **2002**, *84*, 1701.
27. Matsuyama, H.; Maki, T.; Teramoto, M.; Asano, K. *J. Membr. Sci.* **2002**, *204*, 323.
28. Matsuyama, H.; Teramoto, M.; Kudari, S.; Kitamura, Y. *J. Appl. Polym. Sci.* **2001**, *82*, 169.
29. Atkinson, P. M.; Lloyd, D. R. *J. Membr. Sci.* **2000**, *171*, 1.
30. Matsuyama, H.; Yuasa, M.; Kitamura, Y.; Teramoto, M.; Lloyd, D. R. *J. Membr. Sci.* **2000**, *179*, 91.
31. Matsuyama, H.; Teramoto, M.; Kuwana, M.; Kitamura, Y. *Polymer* **2000**, *41*, 8673.
32. Funk, C. V.; Beavers, B. L.; Lloyd, D. R. *J. Membr. Sci.* **2008**, *325*, 1.
33. Yave, W.; Quijada, R. *Desalination* **2008**, *228*, 150.
34. Jeon, M. Y.; Kim, C. K. *J. Membr. Sci.* **2007**, *300*, 172.
35. Luo, B.; Li, Z.; Zhang, J.; Wang, X. L. *Desalination* **2008**, *233*, 19.
36. Chen, G.; Lin, Y. K.; Wang, X. L. *J. Appl. Polym. Sci.* **2007**, *105*, 2000.
37. Lin, Y. K.; Chen, G.; Yang, J.; Wang, X. L. *Desalination* **2009**, *236*, 8.
38. Yang, J.; Li, D. W.; Lin, Y. K.; Wang, X. L.; Tian, F.; Wang, Z. *J. Appl. Polym. Sci.* **2008**, *110*, 341.
39. Han, S.; Woo, S.; Kim, D.; Park, O. O.; Nam, S. *Macromol. Res.* **2014**, *22*, 618.
40. Li, Q.; Bi, Q. Y.; Lin, H. H.; Bian, L. X.; Wang, X. L. *J. Membr. Sci.* **2013**, *427*, 155.
41. Wickramanayake, S.; Hopkinson, D.; Myers, C.; Sui, L.; Luebke, D. *J. Membr. Sci.* **2013**, *439*, 58.
42. Li, Q.; Zhou, B.; Bi, Q. Y.; Wang, X. L. *J. Appl. Polym. Sci.* **2012**, *125*, 4015.
43. Yang, Z. S.; Li, P. L.; Xie, L. X.; Wang, Z.; Wang, S. C. *Desalination* **2006**, *192*, 168.

44. Ji, G. L.; Du, C. H.; Zhu, B. K.; Xu, Y. Y. *J. Appl. Polym. Sci.* **2007**, *105*, 1496.
45. Yoo, S. H.; Kim, C. K. *J. Appl. Polym. Sci.* **2008**, *108*, 3154.
46. Li, N.; Xiao, C.; Wang, R.; Zhang, S. *J. Appl. Polym. Sci.* **2012**, *124*, E169.
47. Tang, Y. H.; He, Y. D.; Wang, X. L. *J. Membr. Sci.* **2012**, *409*, 164.
48. Hołda, A. K.; Vankelecom, I. F. J. *J. Membr. Sci.* **2014**, *450*, 499.
49. Kim, I.; Lee, K. *J. Appl. Polym. Sci.* **2003**, *89*, 2562.
50. Ji, G. L.; Zhu, B. K.; Cui, Z. Y.; Zhang, C. F.; Xu, Y. Y. *Polymer* **2007**, *48*, 6415.
51. Chen, J.; Yan, X.; Chi, X.; Wu, X.; Zhang, M.; Han, C.; Hu, B.; Yu, Y.; Huang, F. *Polym. Chem.* **2012**, *3*, 3175.
52. Su, Y.; Chen, C.; Li, Y.; Li, J. *J. Macromol. Sci. A* **2007**, *44*, 305.
53. Lloyd, D. R.; Kim, S. S.; Kinzer, K. E. *J. Membr. Sci.* **1991**, *64*, 1.
54. Ma, W. Z.; Chen, S.; Zhang, J.; Wang, X. L.; Miao, W. *J. Appl. Polym. Sci.* **2009**, *111*, 1235.
55. Kim, S. S.; Lloyd, D. R. *Polymer* **1992**, *33*, 1036.
56. Lim, G. B. A.; Lloyd, D. R. *Polym. Eng. Sci.* **1993**, *33*, 529.
57. Liang, H. Q.; Wu, Q. Y.; Wan, L. S.; Huang, X. J.; Xu, Z. K. *J. Membr. Sci.* **2013**, *446*, 482.
58. Hansen, C. M. Hansen Solubility Parameter; CRC Press: Boca Raton, **2007**.
59. Grulke, E. A. Polymer Handbook; Brandrup, J.; Immergut, E. H.; Grulke, E. A., Eds.; Wiley: New York, **1999**.
60. Pinnau, I.; Freeman, B. D. Membrane Formation and Modification; Pinnau, I.; Freeman, B. D., Eds.; American Chemical Society: Washington D.C., **1999**.
61. Ma, W. Z.; Zhang, J.; Van der Bruggen, B.; Wang, X. L. *J. Appl. Polym. Sci.* **2013**, *127*, 2715.
62. Tang, Y. H.; Lin, Y. K.; Ma, W. Z.; Tian, Y.; Yang, J.; Wang, X. L. *J. Appl. Polym. Sci.* **2010**, *118*, 3518.
63. Kim, W. K.; Char, K.; Kim, C. K. *J. Polym. Sci., Part B: Polym. Phys.* **2000**, *38*, 3042.
64. Lu, X.; Li, X. *J. Appl. Polym. Sci.* **2009**, *114*, 1213.
65. Liu, T. Y.; Zhang, R. X.; Li, Q.; Van der Bruggen, B.; Wang, X. L. *J. Membr. Sci.* **2014**, *472*, 119.